© 2013 Science Wise Publishing & DE GRUYTER DOI 10.1515/nanoph-2012-0040 — Nanophotonics 2013; 2(2): 153–160

Monan Liu, Rui Chen, Giorgio Adamo, Kevin F. MacDonald, Edbert J. Sie, Tze Chien Sum, Nikolay I. Zheludev, Handong Sun* and Hong Jin Fan*

Tuning the influence of metal nanoparticles on ZnO photoluminescence by atomic-layer-deposited dielectric spacer

Abstract: There is increasing interest in tuning the optical and optoelectronic properties of semiconductor nanostructures using metal nanoparticles in their applications in light-emitting and detection devices. In this work we study the effect of a dielectric Al_2O_3 gap layer (i.e., spacer) on the interaction of ZnO nanowires with metal nanoparticles. The Al_2O_3 spacer thickness is varied in the range of 1–25 nm using atomic layer deposition (ALD) in order to tune the interaction. It is found that ~5 nm is an optimum spacer thickness common for most metals, although the enhancement ratio of the near-bandedge emission differs among the metals. Consistent results are obtained from both photoluminescence (PL) and cathodoluminescence (CL) spectroscopies, with the latter being applied to the optical properties of individual semiconductor/metal nanoheterostructures. The interaction is primarily proposed to be related to coupling of ZnO excitons with local surface plasmons of metals, although other mechanisms should not be ruled out.

Keywords: ZnO nanowires; surface plasmons; metal nanoparticles; photoluminescence; cathodoluminescence; atomic layer deposition.

PACS: 78.67.-n; 78.55.-m; 78.60.Hk; 78.67.Uh.

***Corresponding authors: Handong Sun and Hong Jin Fan,** Division of Physics and Applied Physics, School of Physical and Mathematical Sciences, Nanyang Technological University, 21 Nanyang Link, 637371, Singapore; and Centre for Disruptive Photonic Technologies, Nanyang Technological University, 637378, Singapore, e-mail: hdsun@ntu.edu.sg; fanhj@ntu.edu.sg

Monan Liu, Rui Chen, Edbert J. Sie and Tze Chien Sum: Division of Physics and Applied Physics, School of Physical and Mathematical Sciences, Nanyang Technological University, 21 Nanyang Link, 637371, Singapore

Giorgio Adamo and Nikolay I. Zheludev: Optoelectronics Research Centre and Centre for Photonic Metamaterials, University of Southampton, Highfield, Southampton, SO17 1BJ, UK; and Centre for Disruptive Photonic Technologies, Nanyang Technological University, 637378, Singapore

Kevin F. MacDonald: Optoelectronics Research Centre and Centre for Photonic Metamaterials, University of Southampton, Highfield, Southampton, SO17 1BJ, UK

Tze Chien Sum: Singapore-Berkeley Research Initiative for Sustainable Energy (SinBeRISE), 1 Create Way, Singapore 138602

Edited by Volker Sorger

1 Introduction

Radiative coupling between surface plasmons (SPs) and excitons in a nanoscale optical emitter can lead to fundamental quantum optical phenomena, such as the Purcell effect [1] and vacuum Rabi or normal mode splitting [2–4]. SPs can increase the density of states and thus the spontaneous emission rate in semiconductors [5–8]. Modulations of the spontaneous emission in this SP coupling regime have been successfully realized in various quantum optical systems [9–13]. Semiconductor-dielectric-metal trilayers are archetypal systems for the study of exciton-plasmon-polaritons [14] or exciton-plasmon conversion [15], as well as enhancement of spontaneous light emissions in, e.g., InGaN [10, 16]. In such systems the sandwiched dielectric layer modulates the coupling strength between the two semiconductor excitons and metal SPs due to wave function overlap.

As a typical semiconductor emitter, ZnO has a direct band gap of 3.37 eV and a large exciton binding energy of 60 meV at room temperature. Well-aligned ZnO nanowires (NWs) are being widely studied for their application in light emitting diodes, UV optical switches, and nanoscale lasers [17]. As-grown ZnO NWs usually have a high density of defects or impurities which will trap carriers and result in low luminescence efficiency [18, 19]. Recently, a number of groups have reported that, by coating ZnO with either a metal or dielectric layer, the near-bandgap emission (NBE) intensity can be either increased [20–26], or quenched [27–29]. In particular, direct metal capping appears to be an effective way of enhancing the NBE due to SP coupling [20–23, 26, 30–33]. At the same time, the direct contact of metal with ZnO complicates the interpretation of the

interaction mechanism. A number of possible physical processes could occur at the metal-ZnO interface including, for example, charge transfer [24, 28, 29, 34], unintentional H doping [35], metal-induced gap states [36], and metal diffusion [37]. It is known that in exciton-plasmon coupling for enhancement of fluorescence, a dielectric spacer layer is usually necessary to prevent emission quenching caused by coupling to lossy surface waves. An insulating dielectric layer inserted between ZnO and the metal layer, as adopted in the present study, will retard direct electron flow, and therefore be more appropriate for the study of exciton-plasmon coupling. So far there are limited studies dedicated to the localized SP-coupling-induced enhancement of ZnO luminescence. Lawrie and co-workers studied the effect of MgO spacers on the coupling of SP polaritons on Ag films with polycrystalline ZnO films, and established Purcell enhancement of NBE as well as visible band enhancement through dipole-dipole scattering [38, 39]. Very recently, Liu and co-workers reported the effects of Ag localized SPs on the UV electroluminescence from ZnO/GaN heterojunction light-emitting diodes by inserting MgO spacer layers, and found a similar enhancement trend [40]. No systematic investigation on the spacer-thickness dependence of the luminescence of ZnO NWs has previously been reported.

To realize a homogeneous coating of NWs with a dielectric spacer in this work, we applied atomic layer deposition (ALD) to achieve fine control over the Al_2O_3 spacer thickness for ZnO NW/plasmonic metal nanoparticle heterostructures. It is found, in complementary photo- and cathodoluminescence spectroscopic studies (of NW arrays and singular semiconductor/metal heterostructures, respectively) that the NBE can either be enhanced or quenched depending on the spacer thickness, and a maximum metal nanoparticle-induced enhancement occurs at around 5 nm ALD Al_2O_3. This observation (peak PL enhancement around spacer thickness of 5 nm) is proposed to be a result of competition of a nanoscale hybrid plasmonic mode with other emission mechanisms [41].

2 Experiments

2.1 Sample preparation

Well-aligned ZnO NW arrays were grown from thoroughly mixed ZnO-graphite source powders on gold-coated GaN/*a*-plane sapphire substrates via chemical vapor deposition. Full details of the growth process can be found in Ref. [42]. The as-grown samples were cut into small pieces for subsequent depositions of Al_2O_3 and metal. Coating with Al_2O_3 to the desired thickness was realized by ALD (Beneq TFS-200), using trimethylaluminum (TMA) and water as the aluminum and oxygen sources respectively, at 200°C with a film growth rate of ~0.13 nm/cycle. The thickness was determined based on the linear growth rate. The outer layers of metal nanoparticles were applied via DC sputtering (JFC-1600, JEOL). Some samples were directly sputtered with Au without the intermediate Al_2O_3 spacer for control experiments. The morphology of the NWs was observed using both scanning electron microscope (SEM) and transmission electron microscope (TEM).

2.2 Photoluminescence characterization

Room-temperature PL measurements were carried out using the 325 nm line of a continuous-wave He-Cd laser for excitation at an incident angle of 45° and spectra were recorded in the surface-normal direction. The laser power was 10 mW and the spot size around 1 mm^2. At least three measurements were taken on each sample at different locations on the surface to verify uniformity.

2.3 Cathodoluminescence characterization

The excitation of NWs for CL measurements was performed using an SEM (CamScan CS3200 with LaB6 cathode). All CL measurements were performed by exciting the sample with a 30 kV electron beam at a beam current of ~1.2 nA. Acquisition times varied from 0.01 to 0.5 s depending on the signal intensity: times of 0.5, 0.1 and 0.01 s were used for pristine ZnO NWs, ZnO/Al_2O_3/Pt, and ZnO/Al_2O_3/Au NWs, respectively. The electron beam was focused onto the sample through a small hole in a short-working-distance parabolic mirror mounted directly above the sample, which collected emitted light over approximately half of the available hemispherical solid angle. The mirror directs the light out of the SEM chamber to a hyperspectral light collection system (spectrometer and liquid-nitrogen-cooled CCD detector). This arrangement allows one to build CL maps of the NWs with combined spatial and spectral information about the sample (each point in the map, which has a spatial resolution of ~20 nm, contains the full spectrum of the emitted light) [43, 44].

3 Results and discussion

Vertically aligned ZnO NWs, with a diameters in the range of 80–140 nm and a typical height of 1 μm, are fabricated

via epitaxial growth on lattice-matching GaN layers. As-grown ZnO NWs have very smooth surfaces, which are maintained after application of Al_2O_3 spacer layers by virtue of the ALD process. After metal sputtering, the NW surfaces are decorated with a discontinuous layer of nanoparticles, as shown in Figure 1. In this example the gold nanoparticle diameter is about 5 nm (produced by sputtering at 10 mA for 20 s); the metal particle size increases with higher sputtering currents and/or longer sputtering times.

Figure 2 presents a comparison of the PL spectra from various stages of the NW production and coating process: for a pristine ZnO NW array; a ZnO NW array coated by ALD with Al_2O_3; an array coated with an Al_2O_3 spacer layer and metal nanoparticles; and an array coated directly with metal nanoparticles (i.e., without an Al_2O_3 spacer). Results are presented here for gold nanoparticles, but the pattern of behavior is similar for other metals. The as-grown, pristine ZnO NWs exhibit extremely weak UV emission at 378 nm and strong broadband defect emission centered at 510 nm. This is likely due to a high density of surface defect states within the bandgap, which leads to strong band bending and a significant reduction in the rate of radiative exciton recombination [8, 18, 41]. After coating with Al_2O_3, the visible defect-related emission is somewhat suppressed, while the level of UV emission remains unaffected. In previous PL studies of thinly Al_2O_3- or polymer-coated ZnO NWs [25, 45], a surface passivation effect was proposed to explain a slight enhancement of UV emission with or without a decrease in visible emission. In the present study, the PL spectra show only a slight change in NBE after Al_2O_3 or direct metal coating, indicating that surface passivation is a marginal effect in relation to the optical properties.

When the NWs are directly coated with Au nanoparticles, the UV emission of the ZnO/Au structures is enhanced slightly while the visible emission is drastically quenched. This is consistent with previous reports on direct metal capping of ZnO nanostructures [26, 30, 34]. Finally, the ZnO/Al_2O_3/Au samples present a UV peak that is significantly enhanced at an optimal dielectric thickness of 5 nm. This gigantic increase in the NBE intensity is also observed for other metals (Al, Ag and Pt).

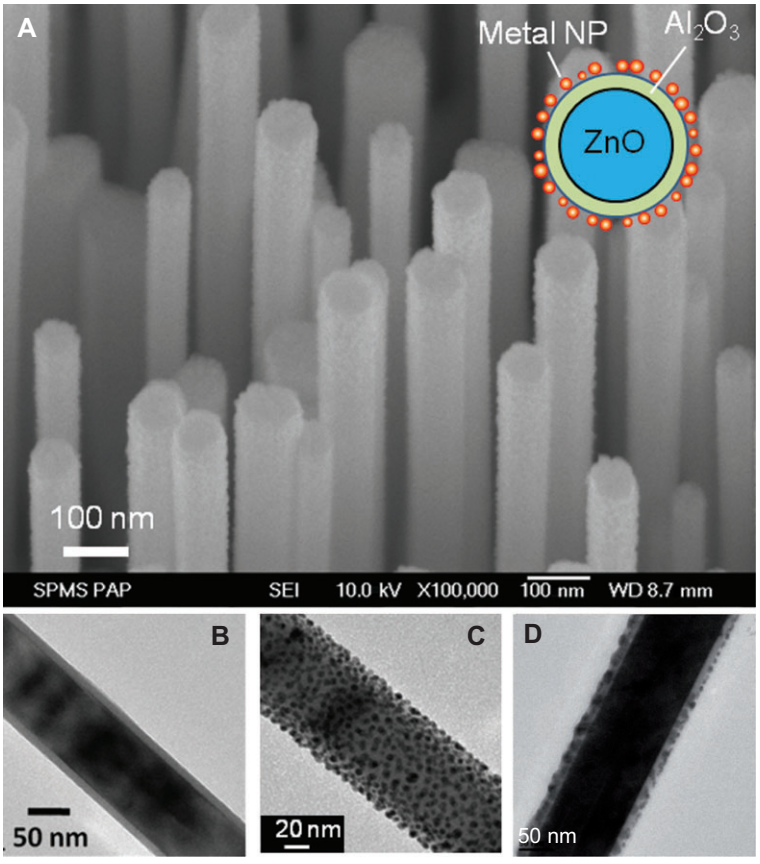

Figure 1 Structure of the semiconductor/dielectric/metal array based on ZnO NWs. (A) SEM image of ZnO/Al_2O_3 5 nm/Au trilayer NW array. Inset is the cross-sectional schematic of a NW. (B) TEM image of a single NW after Al_2O_3 coating by ALD, revealing its smooth surface. (C) TEM image of the ZnO/Al_2O_3 5 nm/Au NW array. (D) TEM image of the ZnO/Al_2O_3 5 nm/Ag NW array.

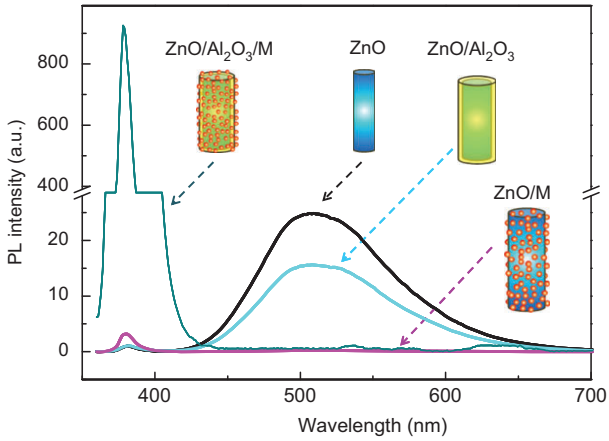

Figure 2 Comparison of PL spectra for ZnO NWs at different stages of the growth/coating process (as labeled). The 5 nm Al_2O_3 layer is applied by atomic layer deposition, and the metal nanoparticles (M=Au, Ag, Pt, Al) by sputtering. The spectra are obtained under identical measurement conditions. Those shown here correspond to gold (M=Au), but the picture is similar for other metals.

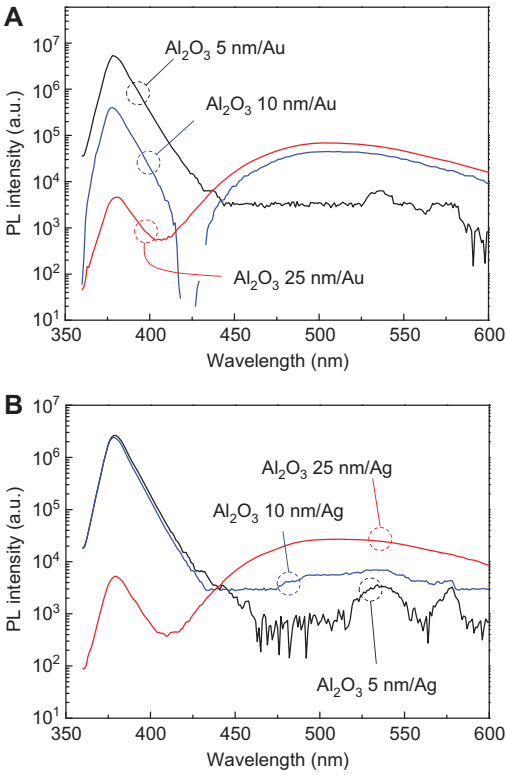

Figure 3 PL spectra of ZnO/Al_2O_3/metal NWs with different ALD Al_2O_3 spacer thicknesses. The outmost layer of sputtered metal is gold for (A) and Ag in (B).

The defect-related surface states of the as-grown ZnO NWs cause strong band bending and charge depletion, therefore reducing the chances for exciton recombination near the surface. With Al_2O_3/metal coating, the defect emissions are reabsorbed by the metals, and simultaneously the plasmon/exciton coupling increases the recombination probability between electrons outside the depletion region and holes within the depletion region.

It is found that the broad visible emission of as-grown ZnO NWs is almost completely eliminated when the metal nanoparticle layer is present, with or without the ALD spacer. The quenching is independent of the thickness of the Al_2O_3 spacer from 0 to at least 25 nm (see more below), indicating that the mechanism responsible for the quenching of visible emissions is not related to SP coupling, but more likely to metal plasmonic absorption. As the metal nanoparticles have a broad plasmonic absorption peak covering the visible range, the ~500 nm emissions from the ZnO NW core can be absorbed by the metal particles.

In order to systematically study the thickness effect of the spacer layer on UV emission, ZnO NWs were coated with different ALD Al_2O_3 spacer thicknesses (5, 10 and 25 nm) and sputter-coated with one of four different metals. To ensure comparability across the samples, each batch of samples were cut from the same pristine ZnO NW sample. Data for gold and silver are presented in Figure 3 (semi-log scale), as they are the two metals of most common interest. The spectra for Pt and Al show very similar trends and thus not presented herein. It is found that the enhancement of UV emissions is most significant at an Al_2O_3 thickness of ~5 nm for all metals; further increase to 10 and 25 nm results in sharp reduction of emission intensity. Table 1 lists the enhancement ratios (defined as the ratio of UV emission intensity of the Al_2O_3/metal-coated NWs to that of the pristine ZnO NWs) for the four types of metal at the spacer thickness of g=5 nm. Substantial PL enhancement in ZnO and other wide bandgap semiconductors by Ag and Al plasmons has been observed previously [10, 40]. Maximum enhancement is expected for resonant coupling between metal SPs and ZnO excitons when the plasmon frequency lies near 3.3 eV (380 nm). For Ag and Al which have localized plasma frequencies in the near UV range, the enhancement ratios are expected to be greater than for Au and Pt, which is not exactly the case in Table 1. The most likely reason for this discrepancy is the different particle size. Although the metals were sputtered under the same condition, the nanoparticle sizes and associated UV extinction coefficients vary significantly from one to the next (the particle sizes roughly estimated from TEM images are ~5 nm for Au, 15 nm for Ag, and 3 nm for Pt. As for Al, the size is indistinguishable probably because of oxidation). The observed PL enhancement of Al is nearly 10 times that of other metals. This could be related to the

Table 1 Relative UV emission intensities of the metal-coated ZnO NWs with respect to that of pristine ZnO NWs. The ALD Al_2O_3 spacer layer thickness is g=5 nm for all metals.

Metal type	Au	Pt	Ag	Al
Enhancement ratio	590	470	420	3960

natural oxidation of the Al nanoparticles, which added an extra Al_2O_3 layer surrounding the Al core and gave an extra enhancement.

To further examine how sensitively the enhancement depends on Al_2O_3 spacer thickness, and to check if there exists a competing passivation effect at small (g<5 nm) Al_2O_3 thickness, a set of control samples with the same gold nanoparticles but different Al_2O_3 thicknesses were prepared and characterized by PL spectroscopy. Figure 4 shows the UV peak intensity increases monotonically with increasing spacer thickness in the range of g=1–5 nm, with the visible emission being heavily suppressed in all cases.

Combining the two sets of g-dependent data above generates the plot shown in inset Figure 4. A transition of the enhancement ratios occurs near g=5 nm, which is a very similar trend to that observed by Sorger et al. in the spacer thickness dependence of PL enhancement due to coupling with the waveguide plasmonic mode [41]. In the Sorger work, dye molecules were placed inside a nanowire-film spacer with high optical localization, and the PL from the molecules formed a hybrid plasmonic polariton (HPP) waveguide mode. The PL enhancement peaked around g=10 nm because of a dominating nanoscale HPP mode over other emission channels, and quenching at smaller g [41]. In our case, although the exact mechanism for the PL enhancement may differ from Sorger et al. the observed shape in Figure 4 (inset) can also be qualitatively explained by two competing effects: i) enhancement of the spontaneous emission rate with decreasing spacer thickness, and ii) an monotonically increasing coupling probability with increasing spacer thickness. The modal Purcell factor is the product of both and hence explains the maximum PL enhancement around 5 nm. The enhancement ratios approach zero at large (g>10 nm) spacer thickness, which, as expected, can be understood by the evanescent nature of the electric field of the SPs across the dielectric layer.

To complement PL studies of NW arrays, CL spectroscopy was employed to investigate the spatially-resolved luminescence properties of individual NWs (Figure 5). The versatility and high spatial-resolution of CL spectroscopy has established it as a powerful tool in the field of nanophotonics [46, 47], plasmonics [44, 48, 49], and more recently metamaterials [50]. The NWs were transferred

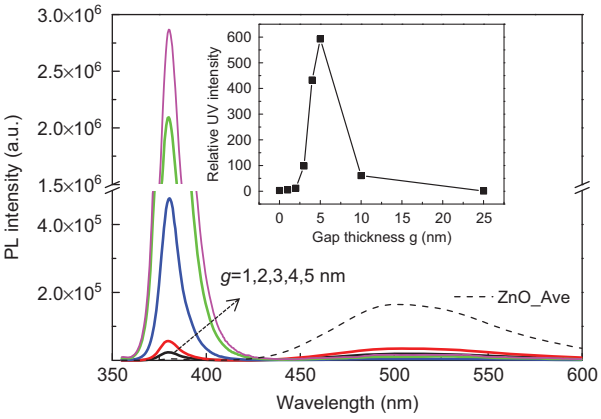

Figure 4 PL spectra of ZnO/Al_2O_3/Au NWs with the ALD Al_2O_3 spacer thicknesses (g) of about 1, 2, 3, 4, and 5 nm. Inset is the plot of the relative UV peak intensity as a function of the gap thickness in the range of 0-25 nm (Data of g=10 and 25 nm are taken from Figure 3A). The solid line is a guide to the eye.

from the growth substrates (GaN/sapphire) into an ethanol solution and then dispersed on Si substrates. To ensure consistency of electron beam excitation conditions for CL analysis, both as-grown ZnO and metal-capped ZnO NWs with Al_2O_3 spacers were dispersed on the same Si substrate (see Figure 5A). CL spectra and corresponding intensity maps for bare ZnO NWs, ZnO NWs coated with 5-nm Al_2O_3/Pt, and ZnO NWs coated with 5-nm Al_2O_3/Au are presented in Figures 5D–F. The spectra were calibrated by assuming the intensity is proportional to the spectrum acquisition time. The CL results for individual NWs correspond well with PL data for NW arrays, revealing again the enhancement of UV emission is quenching of visible emission for metal-coated samples. The mapping result shows that defect emission is uniformly excited for electron injection points along the entire length of pristine ZnO NWs, but that UV emission is relatively less uniformly excited for all samples. This may indicate that the visible emissions originate mainly from the intrinsic defects on the NW surface while the UV emission intensity depends on the coating homogeneity of the metal particles.

4 Conclusion

Through a systematic study of the photo- and cathodoluminescence properties of metal-coated ZnO nanowires with an intermediate dielectric (Al_2O_3) spacer, we provide a strategy for tailoring the optical properties of ZnO NWs. Microscopic, spatially resolved cathodoluminescence measurements on individual NWs are entirely consistent

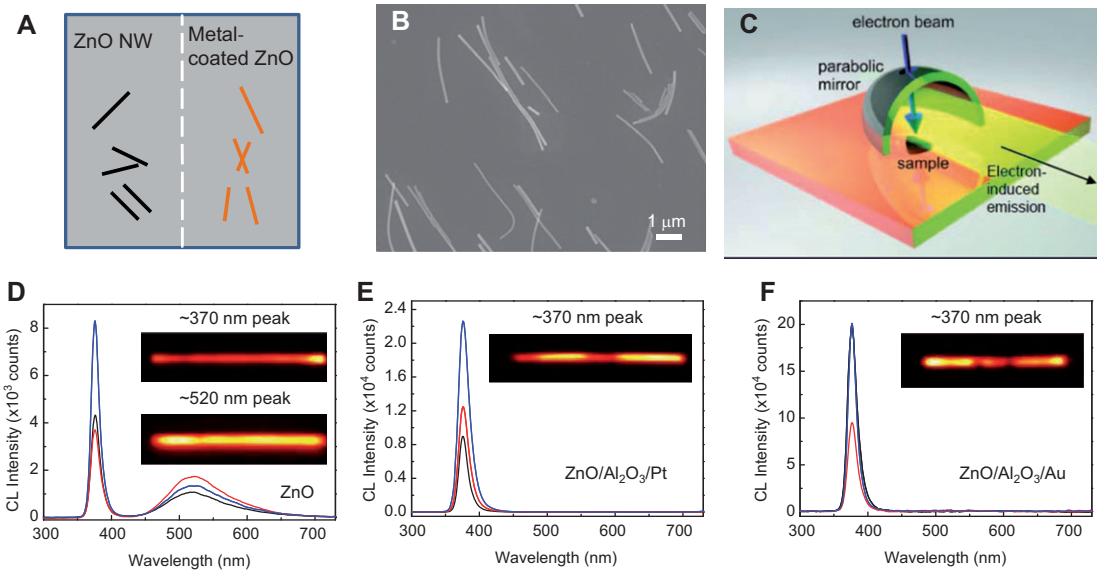

Figure 5 CL emission characterization of individual NWs. (A) Schematics of the CL sample: Si substrates on which with both pristine and Al_2O_3/metal-coated NWs are dispersed and spatially separated. (B) SEM of the dispersed NWs on Si substrate. (C) Schematic of the CL signal collection configuration. (D–F) CL spectra recorded from three locations along the NW length: (D) Pristine ZnO NWs dispersed on a Si substrate, (E) ZnO/Al_2O_3/Pt NWs, and (F) ZnO/Al_2O_3/Au NWs (The Al_2O_3 spacer thickness is 5 nm in all cases.). The insets show corresponding maps of emission intensity as a function of electron injection coordinate.

with macroscopic photoluminescence data for NW arrays. The enhancement of band edge luminescence is found to be highly sensitive to the presence and thickness of the Al_2O_3 spacer: The metal-induced enhancement of UV emission with a dielectric spacer is dramatically larger than the case without spacer, and significant enhancements are obtained at an optimum Al_2O_3 thickness of ~5 nm for the four metals studied (Au, Ag, Al and Pt). This drastic enhancement of NBEs and elimination of defect emissions by metal-dielectric coating ZnO nanowires may have positive effect on their applications in UV detector, light emitting diodes, biosensors, and photovoltaics.

Acknowledgement: This work is supported by the following research grants: Ministry of Education (MOE) Tier 1 grants (M4011011.110, M4010802.110); an NTU start-up grant M4080514.110; a MOE Tier 3 grant, and the Engineering and Physical Sciences Research Council (grant EP/G060363/1).

Received November 28, 2012; accepted March 6, 2013; previously published online March 26, 2013

References

[1] Purcell EM. Spontaneous emission probabilities at radio frequencies. Phy Rev 1946;69:681–1.
[2] Thompson RJ, Rempe G, Kimble HJ. Observation of normal-mode splitting for an atom in an optical cavity. Phys Rev Lett 1992;68:1132–5.
[3] Weisbuch C, Nishioka M, Ishikawa A, Arakawa Y. Observation of the coupled exciton-photon mode splitting in a semiconductor quantum microcavity. Phys Rev Lett 1992;69:3314–7.
[4] Yoshie T, Scherer A, Hendrickson J, Khitrova G, Gibbs HM, Rupper G, Ell C, Shchekin OB, Deppe DG. Vacuum Rabi splitting with a single quantum dot in a photonic crystal nanocavity. Nature 2004;432:200–3.
[5] Hecker NE, Hopfel RA, Sawaki N, Maier T, Strasser G. Surface plasmon-enhanced photoluminescence from a single quantum well. Appl Phys Lett 1999;75:1577–9.
[6] Hobson PA, Wedge S, Wasey JAE, Sage I, Barnes WL. Surface plasmon mediated emission from organic light-emitting diodes. Advanced Materials 2002;14:1393–6.
[7] Kock A, Gornik E, Hauser M, Beinstingl W. Strongly directional emission from AlGaAs/GaAS lighit-emitting-diodes. Appl Phys Lett 1990;57:2327–9.
[8] Anger P, Bharadwaj P, Novotny L. Enhancement and quenching of single-molecule fluorescence. Phys Rev Lett 2006;96:113002
[9] Kulakovich O, Strekal N, Yaroshevich A, Maskevich S, Gaponenko S, Nabiev I, Woggon U, Artemyev M. Enhanced luminescence of CdSe quantum dots on gold colloids. Nano Lett 2002;2:1449–52.
[10] Okamoto K, Niki I, Shvartser A, Narukawa Y, Mukai T, Scherer A. Surface-plasmon-enhanced light emitters based on InGaN quantum wells. Nat Mater 2004;3:601–5.

[11] Song JH, Atay T, Shi SF, Urabe H, Nurmikko AV. Large enhancement of fluorescence efficiency from CdSe/ZnS quantum dots induced by resonant coupling to spatially controlled surface plasmons. Nano Lett 2005;5:1557–61.
[12] Vasa P, Pomraenke R, Schwieger S, Mazur YI, Kunets V, Srinivasan P, Johnson E, Kihm JE, Kim DS, Runge E, Salamo G, Lienau C. Coherent exciton-surface-plasmon-polariton interaction in hybrid metal-semiconductor nanostructures. Phys Rev Lett 2008;101:116801.
[13] Neogi A, Lee CW, Everitt HO, Kuroda T, Tackeuchi A, Yablonovitch E. Enhancement of spontaneous recombination rate in a quantum well by resonant surface plasmon coupling. Physical Review B 2002;66:153305.
[14] Oulton RF, Sorger VJ, Zentgraf T, Ma RM, Gladden C, Dai L, Bartal G, Zhang X. Plasmon lasers at deep subwavelength scale. Nature 2009;461:629–32.
[15] Guo X, Qiu M, Bao JM, Wiley BJ, Yang Q, Zhang XN, Ma YG, Yu HK, Tong LM. Direct coupling of plasmonic and photonic nanowires for hybrid nanophotonic components and circuits. Nano Lett 2009;9:4515–9.
[16] Fedutik Y, Temnov VV, Schops O, Woggon U, Artemyev MV. Exciton-plasmon-photon conversion in plasmonic nanostructures. Phys Rev Lett 2007;99:136802.
[17] Willander M, Nur O, Zhao QX, Yang LL, Lorenz M, Cao BQ, Perez JZ, Czekalla C, Zimmermann G, Grundmann M, Bakin A, Behrends A, Al-Suleiman M, El-Shaer A, Mofor AC, Postels B, Waag A, Boukos N, Travlos A, Kwack HS, Guinard J, Dang DL. Zinc oxide nanorod based photonic devices: recent progress in growth light emitting diodes and lasers. Nanotechnology 2009;20(33):332001.
[18] McCluskey MD, Jokela SJ. Defects in ZnO. Journal of Applied Physics 2009;106:071101.
[19] Zeng HB, Duan GT, Li Y, Yang SK, Xu XX, Cai WP. Blue luminescence of ZnO nanoparticles based on non-equilibrium processes: defect origins and emission controls. Adv Funct Mater 2010;20:561–72.
[20] Lin JM, Lin HY, Cheng CL, Chen YF. Giant enhancement of bandgap emission of ZnO nanorods by platinum nanoparticles. Nanotechnology 2006;17:4391–4.
[21] You JB, Zhang XW, Fan YM, Qu S, Chen NF. Surface plasmon enhanced ultraviolet emission from ZnO films deposited on Ag/Si(001) by magnetron sputtering. Appl Phys Lett 2007;91:231907.
[22] Cheng PH, Li DS, Yuan ZZ, Chen PL, Yang DR. Enhancement of ZnO light emission via coupling with localized surface plasmon of Ag island film. Appl Phys Lett 2008;92:041119.
[23] Li J, Ong HC. Temperature dependence of surface plasmon mediated emission from metal-capped ZnO films. Appl Phys Lett 2008;92:121107.
[24] Li XH, Zhang Y, Ren XJ. Effects of localized surface plasmons on the photoluminescence properties of Au-coated ZnO films. Optics Express 2009;17:8735–40.
[25] Richters JP, Voss T, Wischmeier L, Ruckmann I, Gutowski J. Influence of polymer coating on the low-temperature photoluminescence properties of ZnO nanowires. Appl Phys Lett 2008;92:011103.
[26] Liu KW, Tang YD, Cong CX, Sum TC, Huan ACH, Shen ZX, Wang L, Jiang FY, Sun XW, Sun HD. Giant enhancement of top emission from ZnO thin film by nanopatterned Pt. Appl Phys Lett 2009;94:151102.
[27] Zhou XD, Xiao XH, Xu JX, Cai GX, Ren F, Jiang CZ. Mechanism of the enhancement and quenching of ZnO photoluminescence by ZnO-Ag coupling. Epl 2011;93:57009.
[28] Fang YJ, Sha J, Wang ZL, Wan YT, Xia WW, Wang YW. Behind the change of the photoluminescence property of metal-coated ZnO nanowire arrays. Appl Phys Lett 2011;98:p033103.
[29] Brewster MM, Zhou X, Lu MY, Gradecak S. The interplay of structural and optical properties in individual ZnO nanostructures. Nanoscale 2012;4:1455–62.
[30] Cheng CW, Sie EJ, Liu B, Huan CHA, Sum TC, Sun HD, Fan HJ. Surface plasmon enhanced band edge luminescence of ZnO nanorods by capping Au nanoparticles. Appl Phys Lett 2010;96:071107.
[31] Lai CW, An J, Ong HC. Surface-plasmon-mediated emission from metal-capped ZnO thin films. Appl Phys Lett 2005;86:251105.
[32] Lee MK, Kim TG, Kim W, Sung YM. Surface plasmon resonance (SPR) electron and energy transfer in noble metal-zinc oxide composite nanocrystals. J Physical Chemistry C 2008;112:10079–82.
[33] Lu HF, Xu XL, Lu L, Gong MG, Liu YS. Photoluminescence enhancement of ZnO microrods coated with Ag nanoparticles. J Phys Condes Matter 2008;20:4 (article number: 472202).
[34] Lin HY, Cheng CL, Chou YY, Huang LL, Chen YF, Tsen KT. Enhancement of band gap emission stimulated by defect loss. Optics Express 2006;14:2372–9.
[35] Dev A, Richters JP, Sartor J, Kalt H, Gutowski J, Voss T. Enhancement of the near-band-edge photoluminescence of ZnO nanowires: Important role of hydrogen incorporation versus plasmon resonances. Appl Phys Lett 2011;98:131111.
[36] Richters JP, Dev A, Muller S, Niepelt R, Borschel C, Ronning C, Voss T. Influence of metallic coatings on the photoluminescence properties of ZnO nanowires. Physica Status Solidi-Rapid Research Letters 2009;3:166–8.
[37] Mahanti M, Ghosh T, Basak D. Enhanced near band edge luminescence of Ti/ZnO nanorod heterostructures due to the surface diffusion of Ti. Nanoscale 2011;3:4427–33.
[38] Lawrie BJ, Haglund RF, Mu R. Enhancement of ZnO photoluminescence by localized and propagating surface plasmons. Optics Express 2009;17:2565–72.
[39] Lawrie BJ, Mu R, Haglund RF. Coupling dynamics between photoluminescent centers in ZnO and surface plasmons. Proc of SPIE 2009;7394:73941V-1.
[40] Liu WZ, Xu HY, Zhang LX, Zhang C, Ma JG, Wang JN, Liu YC. Localized surface plasmon-enhanced ultraviolet electroluminescence from n-ZnO/i-ZnO/p-GaN heterojunction light-emitting diodes via optimizing the thickness of MgO spacer layer. Appl Phys Lett 2012;101:142101.
[41] Sorger VJ, Pholchai N, Cubukcu E, Oulton RF, Kolchin P, Borschel C, Gnauck M, Ronning C, Zhang X. Strongly enhanced molecular fluorescence inside a nanoscale waveguide gap. Nano Lett 2011;11:4907–11.
[42] Cheng CW, Liu B, Sie EJ, Zhou WW, Zhang JX, Gong H, Huan CHA, Sum TC, Sun HD, Fan HJ. ZnCdO/ZnO coaxial multiple quantum well nanowire heterostructures and optical properties. J Phys Chem C 2010;114:3863–8.
[43] Bashevoy MV, Jonsson F, MacDonald KF, Chen Y, Zheludev NI. Hyperspectral imaging of plasmonic nanostructures with nanoscale resolution. Optics Express 2007;15:11313–20.

[44] Myroshnychenko V, Nelayah J, Adamo G, Geuquet N, Rodriguez-Fernandez J, Pastoriza-Santos I, MacDonald KF, Henrard L, Liz-Marzan LM, Zheludev NI, Kociak M, de Abajo FJG. Plasmon spectroscopy and imaging of individual gold nanodecahedra: a combined optical microscopy cathodoluminescence, and electron energy-loss spectroscopy study. Nano Lett 2012;12:4172–80.
[45] Liu KW, Chen R, Xing GZ, Wu T, Sun HD. Photoluminescence characteristics of high quality ZnO nanowires and its enhancement by polymer covering. Appl Phys Lett 2010;96:023111.
[46] Tikhomirov VK, Adamo G, Nikolaenko AE, Rodriguez VD, Gredin P, Mortier M, Zheludev NI, Moshchalkov VV. Cathodo- and photoluminescence in Yb3+-Er3+ co-doped PbF2 nanoparticles. Optics Express 2010;18:8836–46.
[47] Sapienza R, Coenen T, Renger J, Kuttge M, van Hulst NF, Polman A. Deep-subwavelength imaging of the modal dispersion of light. Nat Mater 2012;11:781–7.
[48] Denisyuk AI, Adamo G, MacDonald KF, Edgar J, Arnold MD, Myroshnychenko V, Ford MJ, de Abajo FJG, Zheludev NI. Transmitting Hertzian optical nanoantenna with free-electron feed. Nano Lett 2010;10:3250–2.
[49] Frimmer M, Coenen T, Koenderink AF. Signature of a Fano resonance in a plasmonic metamolecule's local density of optical states. Phys Rev Lett 2012;108 (article number: 077404).
[50] Adamo G, Ou JY, So JK, Jenkins SD, De Angelis F, MacDonald KF, Di Fabrizio E, Ruostekoski J, Zheludev NI. Electron-beam-driven collective-mode metamaterial light source. Phys Rev Lett 2012;109:217401.